

# Heparan sulfate on intestinal epithelial cells plays a critical role in intestinal crypt homeostasis via Wnt/ $\beta$ -catenin signaling

Shuji Yamamoto,<sup>1,2</sup> Hiroshi Nakase,<sup>1</sup> Minoru Matsuura,<sup>1</sup> Yusuke Honzawa,<sup>1</sup> Kayoko Matsumura,<sup>1</sup> Norimitsu Uza,<sup>1</sup> Yu Yamaguchi,<sup>3</sup> Emiko Mizoguchi,<sup>4</sup> and Tsutomu Chiba<sup>1</sup>

<sup>1</sup>Department of Gastroenterology and Hepatology, Graduate School of Medicine, Kyoto University, Kyoto; <sup>2</sup>Japan Society for the Promotion of Science, Tokyo, Japan; <sup>3</sup>Sanford Children's Health Research Center, Sanford-Burnham Medical Research Institute, La Jolla, California; <sup>4</sup>Gastrointestinal Unit, Department of Medicine, Massachusetts General Hospital and Harvard Medical School, Boston, Massachusetts

Submitted 18 December 2012; accepted in final form 24 May 2013

**Yamamoto S, Nakase H, Matsuura M, Honzawa Y, Matsumura K, Uza N, Yamaguchi Y, Mizoguchi E, Chiba T.** Heparan sulfate on intestinal epithelial cells plays a critical role in intestinal crypt homeostasis via Wnt/ $\beta$ -catenin signaling. *Am J Physiol Gastrointest Liver Physiol* 305: G241–G249, 2013. First published June 6, 2013; doi:10.1152/ajpgi.00480.2012.—Heparan sulfate (HS), a constituent of HS proteoglycans (HSPGs), is a linear polysaccharide present on the cell surface. HSPGs modulate functions of several growth factors and signaling molecules. We examined whether small intestinal epithelial HS plays some roles in crypt homeostasis using intestinal epithelium cell (IEC)-specific HS-deficient C57Bl/6 mice. Survival rate after total body irradiation was significantly reduced in HS-deficient mice due to profound intestinal injury. HS-deficient IECs exhibited Wnt/ $\beta$ -catenin pathway disruption, decreased levels of  $\beta$ -catenin nuclear localization, and reduced expression of Wnt target genes, including *Lgr5* during crypt regeneration. Moreover, epithelial HS increased Wnt binding affinity of IECs, promoted phosphorylation of Wnt coreceptor LRP6, and enhanced Wnt/ $\beta$ -catenin signaling following ex vivo stimulation with Wnt3a, whereas activation of canonical Wnt signaling following direct inhibition of glycogen synthase kinase-3 $\beta$  by lithium chloride was similar between HS-deficient and wild-type mice. Thus HS influences the binding affinity of IECs to Wnt, thereby promoting activation of canonical Wnt signaling and facilitating regeneration of small intestinal crypts after epithelial injury.

heparan sulfate; intestinal regeneration; Wnt signaling

THE SMALL INTESTINAL EPITHELIUM comprises a single layer of columnar cells that are organized into villi and crypts. Villi extend into the intestinal lumen and contain three types of terminally differentiated cells: enterocytes, goblet cells, and enteroendocrine cells. Enterocytes absorb nutrients, goblet cells secrete mucin, and enteroendocrine cells release gastrointestinal hormones. Crypts are formed by epithelial invaginations into the connective tissue of the intestine and contain stem cells, their transit-amplifying daughter cells, and Paneth cells, which secrete antibacterial peptides into the crypt lumen (99–13). An intricate cell-replacement process maintains the integrity of the mucosal epithelium of the intestine. Vigorous proliferation occurs in crypt compartments. When the committed transit-amplifying cells reach the crypt-villus junction, they rapidly and irreversibly differentiate. The differentiated cells

migrate up to the villus tip, where they are shed. In mouse, the small intestinal epithelium is renewed every 5 days (2).

Several intracellular signaling pathways, such as the Wnt/ $\beta$ -catenin, bone morphogenic protein, phosphoinositide 3-kinase (PI3K)/Akt, and Notch pathways, have critical roles in crypt-villous homeostasis (2). In addition, several extracellular components have also been shown to regulate intestinal crypt homeostasis (36, 39), but their precise roles remain obscure.

Heparan sulfate (HS) is a linear polysaccharide constituting repeating disaccharide units of glucuronic acid and *N*-acetylglucosamine. HS is found on the surface of most cells as a constituent of HS proteoglycans (HSPGs), which comprise a core protein with covalently attached HS chains. In the small intestinal epithelial cells (IECs) of humans (42) and mice (5), HSPGs are predominantly located on the basolateral surface of the cells. HSPGs bind to various growth factors, including Wnt, Hedgehog, transforming growth factor- $\beta$ , and FGF and modulate the biologic activities of these molecules (4, 58).

The importance of HSPG in embryological development is established. In *Drosophila*, HS is required for distribution and signaling of morphogens such as Wingless, Hedgehog, and the *Drosophila* homologue of bone morphogenetic protein, Decapentaplegic, in the embryonic epidermis and the wing disc (8, 20, 22). HS is also involved in FGF signaling during the migration of mesodermal and tracheal cells (32). In vertebrate, HS influences FGF function in zebrafish limb development (40) and is essential for Wnt11 during zebrafish and *Xenopus* gastrulation (41). In mice, HS is required for proper Indian Hedgehog distribution during endochondral bone development (30) and *Fgf8* function in brain development (26). Despite many evidences demonstrating that HSPGs play pivotal roles in embryogenesis, it remains unclear how HSPGs are involved in intestinal epithelial homeostasis.

In the present study, we used the intestine-specific HS-deficient mouse model (5) to elucidate the role of HS in the small intestine.

## MATERIALS AND METHODS

**Mice.** We used C57Bl/6 mice. Conditional *Ext1* allele (*Ext1*<sup>fllox</sup>) was created as described previously (26). *Villin-Cre* mice (16) were obtained from the Jackson Laboratory. Mice were maintained on a 12-h:12-h light/dark cycle and fed standard laboratory mouse chow ad libitum in specific pathogen-free conditions. All experiments were performed with 2- to 4-mo-old mice. All animal experiments in this study were approved by the Review Board of Kyoto University and adhered to their institutional ethical guidelines. For survival data, mice were euthanized if moribund or seriously injured (e.g., vocaliz-

Address for reprint requests and other correspondence: H. Nakase, Dept. of Gastroenterology and Hepatology, Graduate School of Medicine, Kyoto Univ., 54 Shogoin Kawahara-cho, Sakyo-ku, Kyoto, 606-8507, Japan (e-mail: hiroppy\_n@kuhp.kyoto-u.ac.jp)

ing, lack of grooming, or more than 20% weight loss) to prevent suffering.

**Histopathology and immunohistochemical staining.** Mice were killed, and the small intestine was removed, fixed in 10% formaldehyde, and embedded in paraffin. Sections were stained with hematoxylin and eosin reagent. Immunohistochemical staining with anti-HS mAb (10E4; Seikagaku, Tokyo, Japan), bromodeoxyuridine (BrdU) antibody (Sigma-Aldrich, Tokyo, Japan), anti-FGF receptor (FGFR) 1 (phospho Tyr154) antibody (Novus Biologicals, Littleton, CO), or anti-pFGFR3 (Tyr 724) antibody (Santa Cruz Biotechnology, Santa Cruz, CA) was performed on paraffin-embedded slices using the avidin-biotin immunoperoxidase method. Sections were deparaffinized and rehydrated through a graded series of xylene-ethanol washes. Endogenous peroxidase was blocked with 0.3% H<sub>2</sub>O<sub>2</sub>. After biotin was conjugated with secondary antibodies, sections were incubated with the avidin-biotin peroxidase complex (ABC Elite Kit; Vector Laboratories, Burlingame, CA) before reaction with 3,3'-diaminobenzidine/H<sub>2</sub>O<sub>2</sub>. Nuclei were counterstained with hematoxylin. For immunofluorescence staining, specimens were incubated with anti- $\beta$ -catenin antibody (Cell Signaling Technology, Tokyo, Japan) and followed by staining with Alexa Fluor 488 anti-rabbit-IgG (H+L) (Invitrogen, Tokyo, Japan). Nuclei were visualized by DAPI staining.

**Total body  $\gamma$ -irradiation and bone marrow transplantation.** Total body irradiation (TBI) was performed using a <sup>137</sup>Cs source emitting at a fixed-dose rate of 1.11 Gy/min (Gammacell 40 Exactor; MDS Nordion International, Ontario, Canada). For bone marrow transplantation, *Ext1*<sup>fllox/fllox</sup> (*Ext1*<sup>F/F</sup>) donor mice were killed, and marrow cells were harvested from the medullary cavities of the femur by flushing with Hanks' balanced salt solution (GIBCO, Tokyo, Japan). Cells were counted, diluted to  $5 \times 10^6$  cells/200  $\mu$ l, and injected into the tail vein of recipient mice 16 h after TBI. Mice were killed, and the proximal jejunum was rapidly dissected, fixed in 10% neutral buffered formalin, and embedded in paraffin. Paraffin sections (4  $\mu$ m) were cut perpendicular to the long axis of the intestine before immunohistochemical analysis. Immunohistological staining was performed as described above.

**In vivo microcolony assay of crypts.** Crypt stem cell survival was determined 3.5 days after TBI based on BrdU incorporation into proliferating crypt cells, as previously reported (59). Each mouse received 120 mg/kg BrdU intraperitoneally 2 h before harvesting the tissue to permit identification of replicating S phase cells by immunohistochemistry using the avidin-biotin immunoperoxidase method. The number of surviving crypts per cross-section was scored. A surviving crypt was defined as a crypt with five or more BrdU-labeled epithelial cells.

**Isolation of IECs.** IECs were isolated as described previously (27). Mice were killed, and the small intestine was removed and placed in ice-cold PBS flushed through the lumen of the intestines using a syringe. The intestines were then cut longitudinally with scissors and rinsed with cold PBS. The small intestines were placed in PBS with 3 mM EDTA and 50 mM DTT and stored on ice for 1 h in 50-ml conical tubes. The supernatant was filtered and centrifuged for 5 min at 400 g, and the cell pellet was resuspended in cold PBS. Finally, primary IECs were collected by centrifugation through a 20/40% discontinuous Percoll gradient at 600 g for 30 min. Purity of IECs was assessed by flow cytometric analysis using rat anti-mouse E-Cadherin mAb (R & D Systems, Tokyo, Japan) and was confirmed more than 90% pure. Primary mouse IECs were collected in sample buffer for subsequent RNA isolation as well as immunoblotting or in PBS for ex vivo stimulation.

**Immunoblotting.** Primary mouse IECs were lysed with Tris-HCl buffer containing 1% Triton X-100 (lysis buffer). Cell lysate proteins (15  $\mu$ g) were subjected to SDS-PAGE separation followed by immunoblotting using primary antibody. The primary antibodies used for immunoblot analysis were as follows: anti- $\beta$ -catenin, anti-cyclin D1, anti-c-Myc, anti-Survivin, anti-phospho- $\beta$ -catenin (Ser552), anti-Akt,

anti-phospho-Akt (Thr308), anti-Erk1/2, anti-phospho-Erk1/2, anti-SAPK/JNK, anti-phospho-SAPK/JNK, anti-p38 MAPK, anti-phospho-p38 MAPK, anti-phospho-FGF receptor substrate (FRS) 2 $\alpha$ , anti-active  $\beta$ -catenin, anti-LRP6, anti-phospho-LRP6 (Cell Signaling Technology), and anti-Lgr5 antibody (Abcam, Tokyo, Japan). The bound antibody was detected by horseradish peroxidase-conjugated secondary antibody (GE Healthcare, Piscataway, NJ) followed by chemiluminescence using an ECL Plus kit (GE Healthcare). Blotting with anti- $\beta$ -actin antibody (Sigma-Aldrich) was run as a loading control.

**Quantitation of gene expression using real-time PCR.** The total RNA isolated with TRIzol reagent (Invitrogen) was reverse-transcribed using Superscript First-Strand Synthesis System for RT-PCR (Invitrogen) according to the manufacturer's instructions. PCR amplification of cDNA (1  $\mu$ g/20  $\mu$ l of PCR reaction) was carried out in the LightCycler (Roche Diagnostics, Tokyo, Japan) using Fast-Start Universal SYBR Green Master (Rox; Roche Diagnostics). Results are expressed as the ratio of each molecule to *Gapdh*. Primer pairs were as follows: *Gapdh*: AGCCTTCTCCATGGTG-GTGAAGAC (forward), CGGAGTCAACGGATTTGGTCGTAT (reverse); *Lgr5*: CTACTTGACTTTGAGGAAGACC (forward), AG-GAAAGCGCCAGTACTGC (reverse); *cyclin D1*: TCCGCAAGCA TGCACAGA (forward), GGTGGGTTGGAAATGAACCTCA (reverse); *c-Myc*: GCTCGCCAAATCCTGTA (forward), AGGAC-TCGGAGGACAGCA (reverse); *Survivin*: GCGGAGGCTGGC TTCA (forward), AAAAAACACTGGGCCAAATCA (reverse); *Ker-atin8*: TCATCCTATGGGGGACTCAC (forward), TCTTACAAC-CACAGCCTTG (reverse); *Frizzled4*: GACAACCTTCACGCCGC-TCATC (forward), CCAGGCAAACCCAAATTCTCTCAG (reverse); *Frizzled6*: TGTTGGTATCTCTGCGGTCTTCTG (forward), CTCG-CGGCTCTCATTGATG (reverse); *Frizzled7*: ATATCGCCTA-GCAACCACCATCC (forward), AAGGAACGGCACGGAG-GAATG (reverse); and *Axin2*: TCACAGCCCTTGTTGGTTCAAG (forward), GGTAGATTCCTGATGGCCGTAGT (reverse).

**Wnt3a binding assay and ex vivo stimulation of primary mouse IECs.** Recombinant mouse Wnt3a (R&D Systems, Minneapolis, MN) was labeled with Alexa Fluor 488 dye using the Alexa Fluor 488 Microscale Protein Labeling Kit (Invitrogen) according to the manufacturer's instructions. Primary mouse IECs ( $1 \times 10^5$ ) were incubated with 30 ng/ml Alexa Fluor 488-conjugated Wnt3a for 60 min at 37°C. The cells were filtered through nylon filters (Becton Dickinson, Tokyo, Japan) and washed three times with PBS, and mean fluorescent intensity was measured using the FACS Canto II (Becton Dickinson). For ex vivo stimulation, primary mouse IECs were incubated with 30 ng/ml or 100 ng/ml recombinant mouse Wnt3a, 200 ng/ml recombinant mouse Wnt5a (R&D Systems), or 60 mM lithium chloride (LiCl) at 37°C and harvested for immunoblotting or PCR analysis.

**Statistical analysis.** The results are represented as means  $\pm$  SE. A Student's *t*-test was performed for statistical evaluation. Actuarial survival was calculated by the Kaplan-Meier method, and *P* values were evaluated by log-rank test. A *P* value of <0.05 was considered statistically significant.

## RESULTS

**Generation of intestine-specific HS-deficient mice.** To examine whether HS on IEC of the small intestine affects crypt homeostasis, we generated mice with intestine-specific conditional *Ext1* knockout by crossing *Ext1*<sup>F/F</sup> mice with *Villin-Cre* mice as reported previously (5). *Ext1* encodes glycosyltransferase, which polymerizes alternating glucuronic acid and *N*-acetylglucosamine sugar residues in the HS biosynthetic process (35), and is indispensable for HS synthesis because cells lacking a functional *Ext1* allele do not synthesize HS (34,

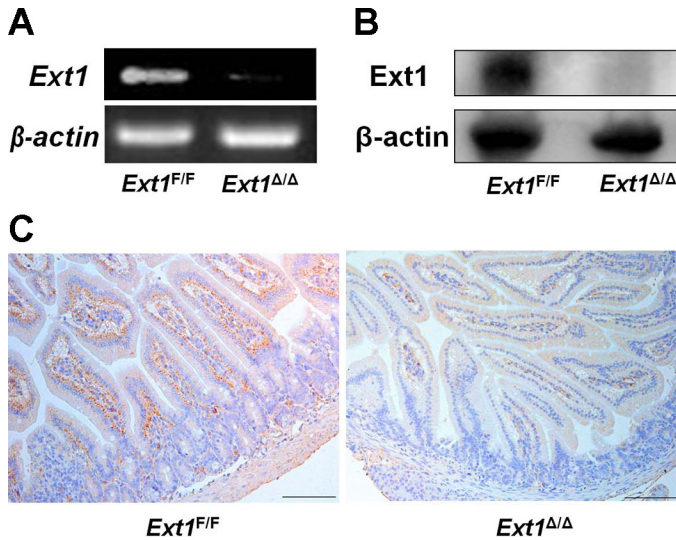


Fig. 1. Heparan sulfate (HS) biosynthesis in intestinal epithelial cells (IECs) was defective in intestine-specific *Ext1*-deficient mice. *A* and *B*: Analysis of PCR products of *Ext1* (*A*) and immunoblotting of *Ext1* (*B*) in IECs isolated from *Ext1*<sup>F/F</sup> and *Ext1*<sup>Δ/Δ</sup> mice. Both mRNA and protein expression of *Ext1* were disrupted in *Ext1*<sup>Δ/Δ</sup> mice. *C*: immunohistochemistry for HS in the small intestine of *Ext1*<sup>F/F</sup> (*left*) and *Ext1*<sup>Δ/Δ</sup> (*right*) mice. Scale bar = 200 μm.

37). Intestine-specific *Ext1* knockout mice are referred to as *Ext1*<sup>Δ/Δ</sup> mice, and *Ext1*<sup>F/F</sup> mice were used as controls.

PCR and immunoblot analyses of IEC separated from the small intestine of *Ext1*<sup>Δ/Δ</sup> mice revealed minimal levels of *Ext1* mRNA (Fig. 1*A*) and *Ext1* protein (Fig. 1*B*), respectively. Immunohistochemical study with a mAb to HS (10E4) revealed that HS was expressed on the basolateral surface of IEC in *Ext1*<sup>F/F</sup> mice (Fig. 1*C, left*), whereas HS expression was undetectable in the IEC of *Ext1*<sup>Δ/Δ</sup> mice (Fig. 1*C, right*). Both macroscopic and microscopic findings were normal in *Ext1*<sup>Δ/Δ</sup> mice as previously reported (5), suggesting that HS on IECs

are not critically involved in crypt homeostasis in the steady state.

*Epithelial HS is required for intestinal regeneration after TBI.* We first examined the effects of intestine-specific deletion of *Ext1* on radiation damage to the small intestine *in vivo*. *Ext1*<sup>F/F</sup> and *Ext1*<sup>Δ/Δ</sup> mice received TBI followed by bone marrow transplantation to rescue from bone marrow death induced by lethal irradiation. Of interest, all *Ext1*<sup>Δ/Δ</sup> mice with 12 Gy TBI died within 6 days despite bone marrow transplantation, whereas 71% of *Ext1*<sup>F/F</sup> mice were alive more than 30 days after TBI (log-rank test;  $P < 0.01$ ; Fig. 2*A*). Histological evaluation 4 days after 12 Gy TBI revealed the small intestinal mucosa with regenerative crypts covering most of the inner intestinal surface in *Ext1*<sup>F/F</sup> mice (Fig. 2*B, top*), whereas severe intestinal damage with almost no villi or crypts in the small intestinal mucosa of *Ext1*<sup>Δ/Δ</sup> mice was observed (Fig. 2*B, bottom*). This finding suggests that *Ext1*<sup>Δ/Δ</sup> mice after TBI died of intestinal damage induced by irradiation. Therefore, we further evaluated roles of epithelial surface HS in crypt regeneration in the small intestine following radiation injury using a crypt microcolony assay (59). Because most of *Ext1*<sup>Δ/Δ</sup> mice died within 4 days after 12 Gy TBI (Fig. 2*A*), dose of irradiation was reduced to 10 Gy in this experiment. Intestine-specific deletion of *Ext1* significantly decreased the number of surviving crypts, which were labeled with BrdU 3.5 days after 10 Gy TBI (Fig. 2, *C* and *D*). Taken together, these results suggest that HS on IECs has protective effects against irradiation and plays critical roles in crypt regeneration after TBI-induced epithelial injury.

*HS is involved in Wnt/β-catenin signaling in intestinal epithelium.* Given that IEC-specific *Ext1* deletion results in decreased proliferation of IECs, we investigated the Wnt/β-catenin and the MAPK pathways that are important for regulating IEC proliferation (17, 50). Immunoblot analysis demonstrated no significant difference in the phosphorylation of the MAPKs, including p38 MAPK, Erk1/2, and JNK1/2, in IECs 4 days after TBI between

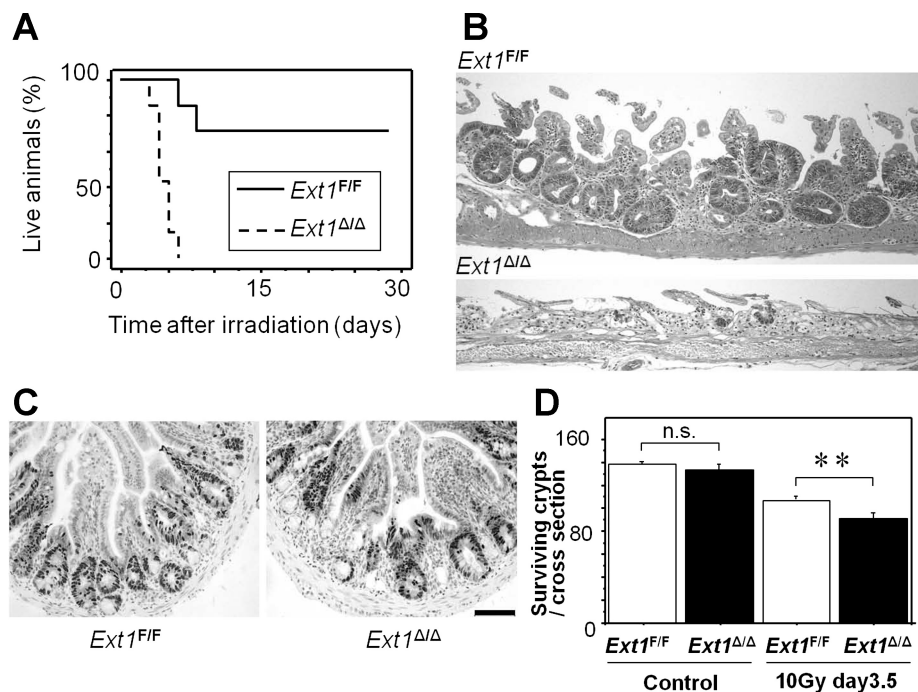
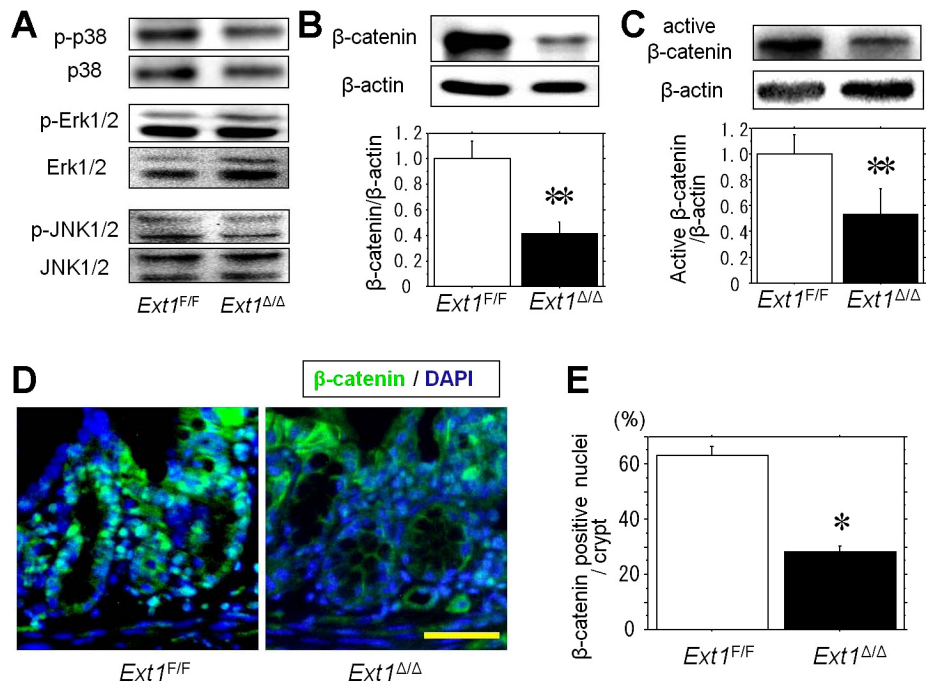


Fig. 2. Intestine-specific HS-deficient mice were sensitive to total body irradiation (TBI)-induced gastrointestinal toxicity. *A*: Kaplan-Meier survival analysis of *Ext1*<sup>F/F</sup> and *Ext1*<sup>Δ/Δ</sup> mice after 12 Gy TBI ( $n = 7$ ). By log-rank test,  $P = 0.0004$ . *B*: upper jejunal sections of *Ext1*<sup>F/F</sup> (*top*) and *Ext1*<sup>Δ/Δ</sup> (*bottom*) mice 4 days after 12 Gy TBI stained with hematoxylin and eosin. *C*: representative bromodeoxyuridine (BrdU) labeling of surviving crypts. Scale bar = 100 μm. *D*: surviving crypts per cross-section. A surviving crypt was defined as a crypt with 5 or more BrdU-labeled epithelial cells. 6 cross-sections per mouse were scored and compared between *Ext1*<sup>F/F</sup> and *Ext1*<sup>Δ/Δ</sup> mice ( $n = 4-6$ ). n.s., not significant,  $**P < 0.05$ .

Fig. 3. The protein levels of total and active  $\beta$ -catenin were decreased in intestine-specific HS-deficient mice after TBI. **A**: immunoblotting analysis of phosphorylated and total MAPKs. A representative blot from 5 independent experiments is shown. **B** and **C**: immunoblotting analysis of total  $\beta$ -catenin (**B**) and activated nonphosphorylated  $\beta$ -catenin (**C**). A representative blot is shown, and graph bars are expressed as the ratio of each molecule to  $\beta$ -actin. ( $n = 5$ )  $**P < 0.05$ . **D**: representative images of immunofluorescence staining for  $\beta$ -catenin in the small intestine of  $Ext1^{F/F}$  and  $Ext1^{\Delta/\Delta}$  mice.  $\beta$ -catenin was stained with Alexa Fluor 488, and nuclei were visualized by DAPI staining. Scale bar = 100  $\mu$ m. **E**: the ratio of crypt cells with  $\beta$ -catenin-positive nucleus per crypt. More than 50 crypts per mouse were scored and compared between  $Ext1^{F/F}$  and  $Ext1^{\Delta/\Delta}$  mice ( $n = 3$ ).  $*P < 0.01$ .



$Ext1^{\Delta/\Delta}$  and  $Ext1^{F/F}$  mice (Fig. 3A). In contrast, the protein levels of total  $\beta$ -catenin were lower in IECs isolated from the small intestine of  $Ext1^{\Delta/\Delta}$  mice 4 days after 10 Gy TBI than those of  $Ext1^{F/F}$  mice (Fig. 3B). In addition, nonphosphorylated  $\beta$ -catenin (active  $\beta$ -catenin) was also lower in  $Ext1^{\Delta/\Delta}$  mice (Fig. 3C). Moreover, immunofluorescence staining revealed lower levels of  $\beta$ -catenin nuclear localization in crypt cells of  $Ext1^{\Delta/\Delta}$  mice 4 days after TBI, compared with those of  $Ext1^{F/F}$  mice (Fig. 3, D and E). These data suggest the decreased

protein levels of cytoplasmic  $\beta$ -catenin with attenuated canonical Wnt signaling in IECs of  $Ext1^{\Delta/\Delta}$  mice after TBI.

To address whether decreased levels of  $\beta$ -catenin had functional consequences, we examined the expression of Wnt target genes including, *cyclin D1*, *c-Myc*, *Survivin*, and *Lgr5*, in IECs isolated from  $Ext1^{F/F}$  and  $Ext1^{\Delta/\Delta}$  mice. Both the mRNA and protein levels of these genes in IECs with disrupted HS biosynthesis were lower than those in HS-competent IECs after TBI (Fig. 4, A and B). To exclude the possibility that reduced

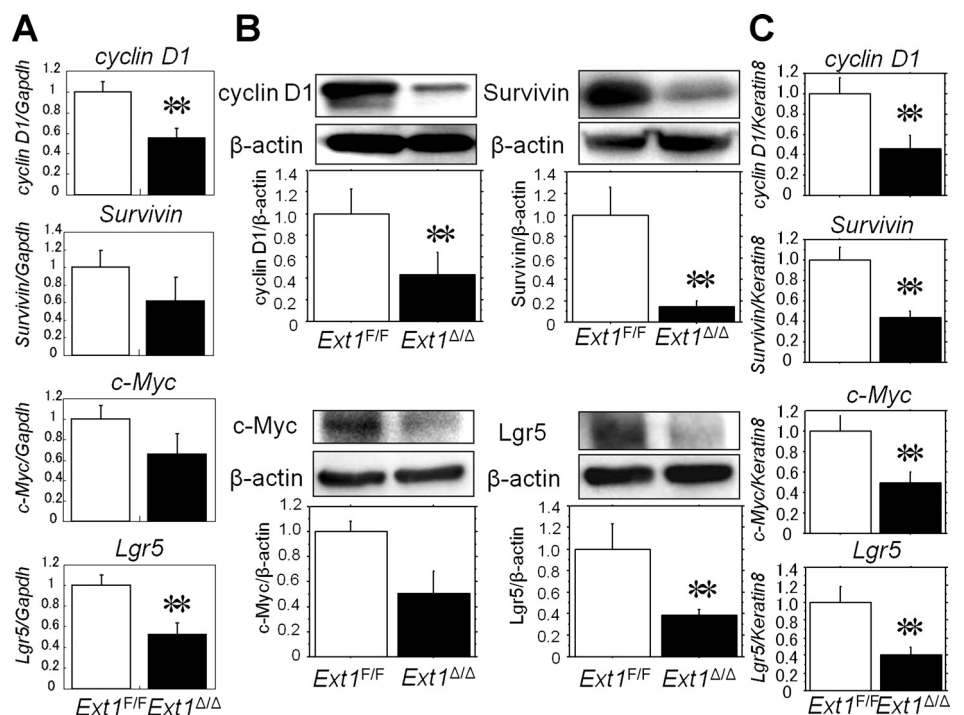


Fig. 4. The mRNA and protein levels of Wnt-target genes were lower in IECs from intestine-specific  $Ext1$  knockout mice than those from  $Ext1^{F/F}$  mice 4 days after 10 Gy TBI. **A**: The mRNA levels of Wnt-target genes *cyclinD1*, *c-Myc*, *Survivin*, and *Lgr5*. Results are expressed as the ratio of each molecule to *Gapdh*. ( $n = 4-7$ )  $**P < 0.05$ . **B**: immunoblotting analysis of Wnt-target genes in IECs from  $Ext1^{F/F}$  and  $Ext1^{\Delta/\Delta}$  mice. A representative blot is shown, and graph bars are expressed as the ratio of each molecule to  $\beta$ -actin. ( $n = 5$ )  $**P < 0.05$ . **C**: mRNA levels of Wnt-target genes normalized by *Keratin8*. ( $n = 4-7$ )  $**P < 0.05$ .

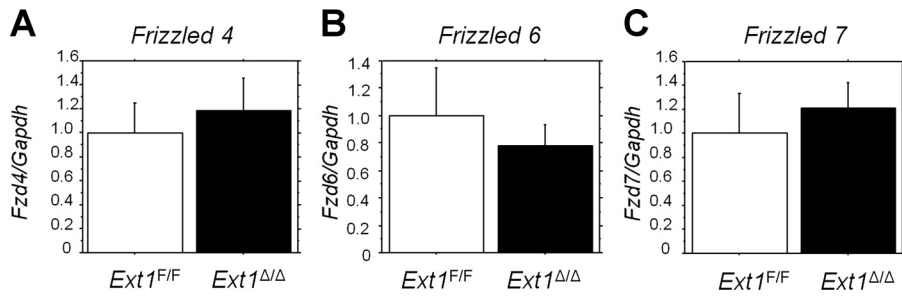


Fig. 5. The gene expressions of *Frizzled4*, 6, and 7 were similar between *Ext1<sup>F/F</sup>* and *Ext1<sup>Δ/Δ</sup>* mice 4 days after 10 Gy TBI. Quantitative PCR analysis of *Frizzled4* (A), 6 (B), and 7 (C). Results are expressed as the ratio of each molecule to *Gapdh*. ( $n = 4-7$ ).

numbers of crypt cells reflected lower levels of expression of Wnt target genes in *Ext1<sup>Δ/Δ</sup>* mice, we used *Keratin8*, the major intermediate filament proteins in the intestinal epithelia (57), to normalize the data in addition to a housekeeping gene. As expected, the mRNA levels of Wnt target genes were significantly lower in IECs harvested from *Ext1<sup>Δ/Δ</sup>* mice than those from *Ext1<sup>F/F</sup>* mice even when normalized by *Keratin8* (Fig. 4C). These data indicate that disruption of *Ext1* in IECs impaired Wnt/ $\beta$ -catenin signaling and that HS plays an important role in regeneration of intestinal crypts following TBI-induced intestinal injury.

In addition, we evaluated the mRNA expression of Frizzled receptors, acting as receptors for Wnt proteins (2, 44, 50), which resulted in similar levels between *Ext1<sup>F/F</sup>* and *Ext1<sup>Δ/Δ</sup>* mice (Fig. 5, A–C).

*Deletion of HS in IECs does not affect the FGF-FGFR axis or the PI3K-Akt pathway.* Next, we investigated the mechanism by which intestinal epithelial HS mediates Wnt/ $\beta$ -catenin signaling. It was recently reported that FGFR3 signaling regulates crypt epithelial stem cell expansion and crypt morphogenesis partly through  $\beta$ -catenin/T cell factor-4-dependent pathways (56). In addition, HS binds to both FGFs and FGFRs (43, 49) and is required for FGF signal transduction (32). Therefore, we first evaluated the FGF-FGFR axis in radiation

enteritis. Immunohistochemical analysis revealed no significant difference in the phosphorylation of FGFR3 and FGFR1 in crypts 4 days after 10 Gy TBI between *Ext1<sup>Δ/Δ</sup>* and *Ext1<sup>F/F</sup>* mice (Fig. 6, A and B). Moreover, levels of phosphorylation of the docking-protein FRS2 $\alpha$ , which plays a critical role in FGFR-mediated signal transduction pathways (19, 21), were similar in IECs between *Ext1<sup>F/F</sup>* and *Ext1<sup>Δ/Δ</sup>* mice (Fig. 6C).

Given that the PI3K-Akt pathway activates Wnt/ $\beta$ -catenin signaling by phosphorylating  $\beta$ -catenin at Ser552 (24, 31), we next examined whether PI3K-Akt pathway-mediated  $\beta$ -catenin activation was involved in the disruption of HS in IECs. Phosphorylation of Akt at Ser 308 was a similar level in IECs of *Ext1<sup>Δ/Δ</sup>* mice and *Ext1<sup>F/F</sup>* mice. In addition, protein levels of phosphorylated  $\beta$ -catenin at Ser552 in IECs from *Ext1<sup>Δ/Δ</sup>* mice were comparable with those from *Ext1<sup>F/F</sup>* mice (Fig. 6D). These data suggest that neither the FGF-FGFR axis nor the PI3K-Akt pathway is involved in HS-dependent Wnt/ $\beta$ -catenin signaling in IECs from HS-deficient mice after irradiation.

*HS affects binding affinity of IECs to Wnt3a and enhanced Wnt/ $\beta$ -catenin signaling.* Because HS chains are capable of binding Wnt proteins (1, 7, 46), we hypothesized that HS on IEC binds Wnt proteins and increases the dose of the ligands on the cell surface, which may result in enhanced Wnt/ $\beta$ -catenin signaling. Therefore, we assessed Wnt3a binding in

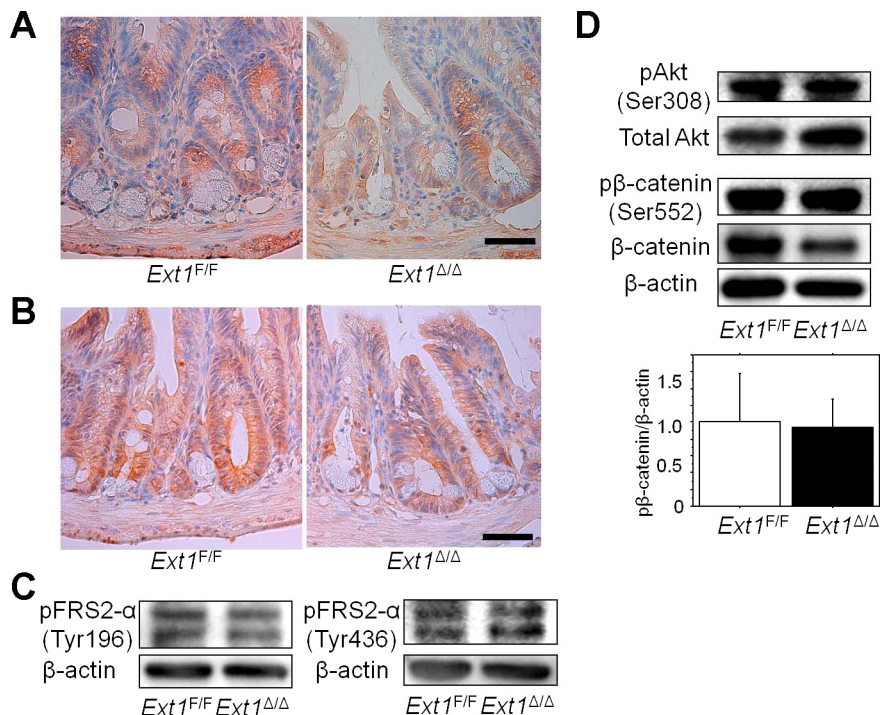


Fig. 6. FGF-FGFR axis and phosphoinositide 3-kinase (PI3K)-Akt pathway were similar between *Ext1<sup>F/F</sup>* and *Ext1<sup>Δ/Δ</sup>* mice 4 days after 10 Gy TBI. A and B: immunohistochemistry for pFGFR3 (A) and pFGFR1 (B) in the small intestine of *Ext1<sup>F/F</sup>* and *Ext1<sup>Δ/Δ</sup>* mice. A representative image from 6 mice is shown. Scale bar = 100  $\mu$ m. C: immunoblotting analysis of phospho-FGFR receptor substrate (pFRS2) $\alpha$  (Tyr196 and Tyr436) in IECs isolated from *Ext1<sup>F/F</sup>* and *Ext1<sup>Δ/Δ</sup>* mice. A representative blot is shown from 5 independent experiments. D: immunoblotting analysis of pAkt,  $\beta$ -catenin (Ser552), and total  $\beta$ -catenin in IECs isolated from *Ext1<sup>F/F</sup>* and *Ext1<sup>Δ/Δ</sup>* mice. A representative blot is shown, and graph bars are expressed as the ratio of each molecule to  $\beta$ -actin. ( $n = 5$ ).

IECs harvested from *Ext1<sup>F/F</sup>* and *Ext1<sup>Δ/Δ</sup>* mice. Flow cytometric analysis indicated that the binding of fluorescent-labeled Wnt3a to IECs of *Ext1<sup>Δ/Δ</sup>* mice was significantly lower than that of *Ext1<sup>F/F</sup>* mice (Fig. 7, A and B). Moreover, immunoblot analysis revealed that stabilization of β-catenin by ex vivo stimulation with Wnt3a was attenuated in IECs from *Ext1<sup>Δ/Δ</sup>* mice compared with *Ext1<sup>F/F</sup>* mice, whereas β-catenin stability was not affected by deletion of HS sugar chains when IECs were incubated with LiCl (Fig. 7C), which directly inhibits the activity of glycogen synthase kinase-3β in a Wnt-independent manner (25, 28). In addition, phosphorylation of Wnt coreceptor LRP6 at Ser 1,490 (2, 44, 50) after ex vivo stimulation with Wnt3a was attenuated in IECs harvested from *Ext1<sup>Δ/Δ</sup>* mice (Fig. 7D). The mRNA levels of Wnt target gene *Axin2* were lower in IECs of *Ext1<sup>Δ/Δ</sup>* mice than those of *Ext1<sup>F/F</sup>* mice after incubation with Wnt3a, and the difference of *Axin2* expression between *Ext1<sup>F/F</sup>* and *Ext1<sup>Δ/Δ</sup>* mice after stimulation with 100 ng/ml of Wnt3a was augmented, whereas similar levels of *Axin2* gene expression were observed between two groups after ex vivo stimulation with LiCl (Fig. 7E). These results suggest that HS on IECs increases cell surface binding affinity of IECs to Wnt ligands, enhances Wnt/β-catenin signaling, and facilitates crypt regeneration after intestinal epithelial injury.

## DISCUSSION

In this study, we showed that intestine-specific HS-deficient mice were more sensitive to TBI-induced intestinal injury than *Ext1<sup>F/F</sup>* mice and that HS influenced Wnt binding affinity of IECs and subsequent Wnt/β-catenin signaling. Our data suggested that HS plays an important role in Wnt/β-catenin signaling during regeneration of the small intestinal crypts in mice.

First, we assessed the role of epithelial HS in regeneration of small intestine after TBI. The gross intestinal phenotype and histology of intestine-specific HS-deficient mice without TBI appeared normal in our study, being in agreement with the findings by Bode et al. (5). However, our study demonstrated that the survival rate of these mice after TBI was significantly reduced compared with that of *Ext1<sup>F/F</sup>* mice due to severe small intestinal injury. Furthermore, in in vivo crypt colony assay, which reflects the capacity of regeneration of intestinal crypts after irradiation (59), the number of surviving crypts in intestine-specific *Ext1*-deficient mice was significantly lower than that in *Ext1<sup>F/F</sup>* mice. These findings suggest that HS is essential for crypt regeneration after intestinal epithelial injury.

Next, we investigated whether HS plays some roles in MAPK pathways or Wnt/β-catenin signaling in IECs. Several

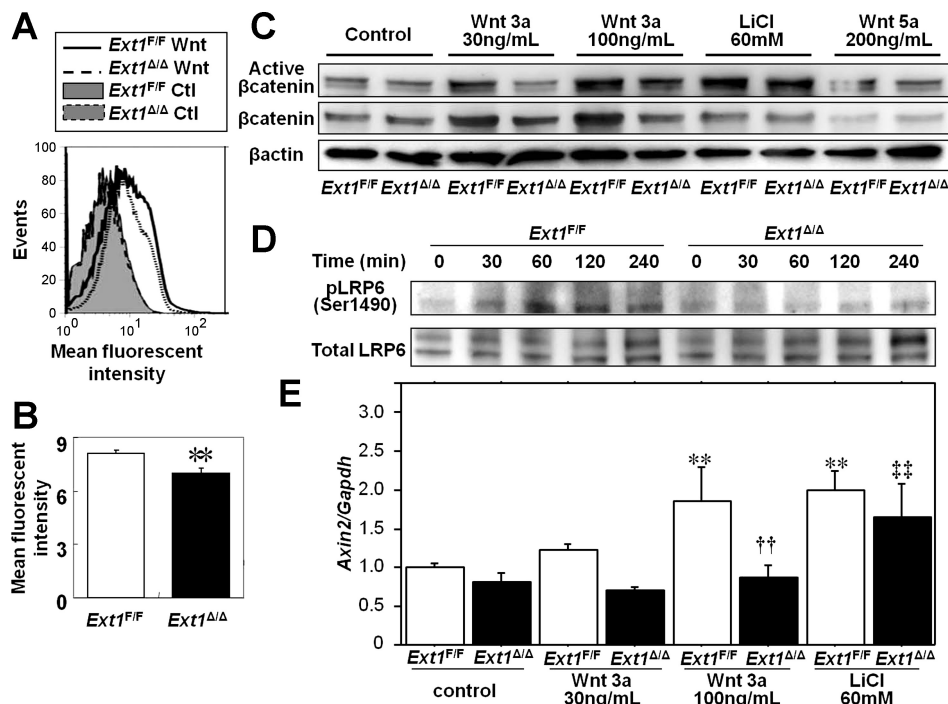


Fig. 7. The binding affinity with Wnt3a was decreased, and Wnt/β-catenin signaling was disturbed in IECs defective in HS biosynthesis in ex vivo stimulation with Wnt3a but not with LiCl. A and B: Wnt3a binding assay of IECs harvested from *Ext1<sup>F/F</sup>* and *Ext1<sup>Δ/Δ</sup>* mice. IECs from *Ext1<sup>F/F</sup>* or *Ext1<sup>Δ/Δ</sup>* mice were incubated with 30 ng/ml Alexa Fluor 488-conjugated Wnt3a for 60 min at 37°C. A: representative flow cytometry histogram. Fluorescent intensities of HS-competent IECs incubated with (*Ext1<sup>F/F</sup>* Wnt; solid line, open histogram) or without (*Ext1<sup>F/F</sup>* Ctl; solid line, solid histogram) Wnt3a and those of HS-deficient IECs with (*Ext1<sup>Δ/Δ</sup>* Wnt; dashed line, open histogram) or without (*Ext1<sup>Δ/Δ</sup>* Ctl; dashed line, solid histogram) Wnt3a are shown. B: mean fluorescence intensity of IECs incubated with fluorescent-conjugated Wnt3a after subtracting that of the untreated IECs ( $n = 3$ ). \*\* $P < 0.05$ . C: immunoblotting analysis of total and active β-catenin in IECs after ex vivo stimulation with Wnt3a, LiCl, or Wnt5a. Primary mouse IECs were incubated with 30 ng/ml or 100 ng/ml Wnt3a, 60 mM LiCl, or 200 ng/ml Wnt5a for 240 min at 37°C and harvested for immunoblotting. Untreated IECs were used as controls. A representative blot from 3 independent experiments is shown. D: immunoblotting analysis of phosphorylated and total LRP6 in IECs after ex vivo stimulation with Wnt3a. IECs from *Ext1<sup>F/F</sup>* or *Ext1<sup>Δ/Δ</sup>* mice were incubated with 100 ng/ml Wnt3a at 37°C and harvested after indicated time for immunoblotting. A representative blot from 3 independent experiments is shown. E: quantitative PCR analysis of *Axin2* in IECs incubated with Wnt3a or LiCl for 240 min. Untreated IECs were used as controls. The gene expressions were normalized by *Gapdh*. ( $n = 6$ ) \*\* $P < 0.05$  compared with *Ext1<sup>F/F</sup>* control; †† $P < 0.05$  compared with *Ext1<sup>F/F</sup>* Wnt3a 100 ng/ml; ‡‡ $P < 0.05$  compared with *Ext1<sup>Δ/Δ</sup>* control.

lines of evidence indicate that MAPK pathways are involved in, not only intestinal cell proliferation, but also intestinal tumorigenesis (17). Our study demonstrated that activation of MAPK pathways in IECs was similar between *Ext1<sup>F/F</sup>* and *Ext1<sup>Δ/Δ</sup>* mice after TBI, suggesting that HS does not play a significant role in MAPK signaling during the regeneration of intestinal crypts after lethal irradiation. In contrast, protein levels of total as well as active form of  $\beta$ -catenin were lower, and  $\beta$ -catenin nuclear localization was reduced in IECs isolated from the small intestine of *Ext1<sup>Δ/Δ</sup>* mice than *Ext1<sup>F/F</sup>* mice. To confirm whether decreased levels of  $\beta$ -catenin had functional consequences, we examined the expression of Wnt target genes in IECs isolated from *Ext1<sup>F/F</sup>* and *Ext1<sup>Δ/Δ</sup>* mice. Expressions of Wnt target genes in IECs in *Ext1<sup>Δ/Δ</sup>* mice were lower than those in *Ext1<sup>F/F</sup>* mice. Thus the Wnt/ $\beta$ -catenin pathway was disturbed, and the expression of Wnt target genes was reduced in HS-deficient IECs. Wnt/ $\beta$ -catenin signaling plays a central role in the regeneration of intestinal epithelium (29, 44). In addition, the role of HSPGs in the regulation of Wnt pathway has been extensively studied in cell signaling during development. In *Drosophila*, the abrogation of HSPG activity by mutation of the EXT family genes leads to reduced extracellular Wingless levels and loss of Wnt target gene expression (6, 23, 52). In *Xenopus*, HSPGs have been shown to interact with Wnt11 during gastrulation (41) and axis formation (53). Taken together, our data and previous findings indicate that HS on IECs has an important function in canonical Wnt signaling and is essential for the proliferation of small intestinal epithelium. Notably, our data demonstrated that both mRNA expression and protein levels of c-Myc and Lgr5 were reduced when intestinal epithelial HS was disrupted. c-Myc is essential for accelerating the cell cycle of crypt progenitor cells (38), and Lgr5 is one of the intestinal stem cell markers (3). These findings may suggest that HS on IEC is required for the expansion of intestinal stem cells, as well as for the proliferation of transit-amplifying cells after crypt injury.

Finally, we examined the effect of HS on cell-binding affinity of Wnt proteins, which may result in enhanced Wnt/ $\beta$ -catenin signaling. Our results revealed that Wnt binding affinity of IECs and Wnt/ $\beta$ -catenin signaling in *ex vivo* stimulation with Wnt3a were clearly reduced by HS deficiency. On the other hand, activation of Wnt/ $\beta$ -catenin signaling following direct inhibition of glycogen synthase kinase-3 $\beta$  by LiCl was not affected by HS deficiency although the possibility cannot be denied that other effects of LiCl than inhibition of glycogen synthase kinase-3 $\beta$ , such as inducing autophagy by inhibiting inositol monophosphatase (48), are influenced. Furthermore, phosphorylation of LRP6 by stimulation with Wnt3a was reduced in IECs from *Ext1<sup>Δ/Δ</sup>* mice. These findings strongly suggest that HS on the cell surface enhanced binding of Wnt ligands to IECs and thereby promoted the canonical Wnt pathway in the regeneration of intestinal epithelium.

Modification of HS structures has been reported to be important for binding to Wnt ligands or receptors. The *Drosophila* mutants of sulfateless, HS *N*-deacetylase/*N*-sulfotransferase, are completely deficient in HS sulfation and have disrupted Wingless signaling (33, 54). Reducing 6-O-sulfation of the HS chains results in the reduction of Wnt binding to HS, facilitating the interaction between Wnt ligand and receptor and promotes canonical Wnt signal transduction (1, 18). Because we disrupted the *Ext1* gene, which is indispensable for

HS synthesis, HS was almost completely eliminated on the surface of IECs in our study. Therefore, specific conformations of HS for binding to Wnt and facilitating ligand-receptor signal transduction in crypt regeneration remain to be elucidated.

Furthermore, in our study, HS synthesis was disturbed irrespective of the family of HSPGs. Cell surface HSPGs are classified into two major families based on their core protein structure, glypicans and syndecans. Glypicans are linked to the plasma membrane by a glycosylphosphatidylinositol linkage and syndecans by a transmembrane domain. Several studies demonstrated that glypicans play an important role in the interaction between HS and Wnt signaling (33, 55), whereas syndecans are important for wound repair (15, 51) and IEC proliferation (14). Further studies are needed to determine which HSPGs are most involved in intestinal crypt regeneration.

Recently, several populations of intestinal stem cells, including Lgr5<sup>+</sup> cells (3), Bmi1<sup>+</sup> cells (47), and Lrig1<sup>+</sup> cells (45), have been identified. Each of these populations has its own distinctive adjacent niches and plays separate but cooperative functions in homeostasis of intestinal crypt (3, 45, 47). In this study, we focused Lgr5 expression in IECs after TBI. At the minimum, our data suggested that gene expression and protein levels of Lgr5 were attenuated in IECs with disrupted HS biosynthesis although there was one limitation that specificity of anti-Lgr5 antibody used in this study was not validated by immunohistochemistry. Thus further investigations on the interaction between HS on IECs and intestinal stem cells would be required.

In conclusion, we elucidated an important role of HS in extracellular regulation of Wnt signaling in crypt regeneration of the small intestine. Further studies on the interactions of HSPGs with Wnt ligands and their receptors will provide new insights into the homeostatic mechanisms of the intestine.

## GRANTS

This work was supported by a Grant-in-Aid for the Japan Society for the Promotion of Science Fellows (to S. Yamamoto); a Grant-in-Aid for Scientific Research (C) from the Ministry of Culture and Science of Japan (grant 18590677), the Kato Memorial Trust for Nambu Research, the Japan Foundation for Applied Enzymology, the Shimizu Foundation for the Promotion of Immunology Research (to H. Nakase); a research grant (ROI DK 80070) from the National Institutes of Health in the U.S. (to E. Mizoguchi); Grants-in-Aid for Scientific Research (16017240, 16017249, 17013051, 17659212, and 18012029) from the Ministry of Education, Culture, Sports, Science, and Technology of Japan, Grants-in-Aid for Scientific Research (15209024 and 18209027) from JSPS, and a Grant-in-Aid for Research on Measures for Intractable Disease, and Research on Advanced Medical Technology (nano005) from the Ministry of Health, Labor, and Welfare, Japan (to T. Chiba).

## DISCLOSURES

No conflicts of interest, financial or otherwise, are declared by the authors.

## AUTHOR CONTRIBUTIONS

Author contributions: S.Y., H.N., and T.C. conception and design of research; S.Y., M.M., Y.H., K.M., N.U., and Y.Y. performed experiments; S.Y., M.M., Y.H., K.M., and N.U. analyzed data; S.Y., H.N., M.M., Y.H., K.M., N.U., Y.Y., E.M., and T.C. interpreted results of experiments; S.Y. prepared figures; S.Y. drafted manuscript; S.Y., H.N., Y.Y., E.M., and T.C. edited and revised manuscript; S.Y., H.N., M.M., Y.H., K.M., N.U., Y.Y., E.M., and T.C. approved final version of manuscript.

## REFERENCES

1. Ai X, Do AT, Lozynska O, Kusche-Gullberg M, Lindahl U, Emerson CP Jr. Qsulf1 remodels the 6-O sulfation states of cell surface heparan

- sulfate proteoglycans to promote Wnt signaling. *J Cell Biol* 162: 341–351, 2003.
2. **Barker N, van de Wetering M, Clevers H.** The intestinal stem cell. *Genes Dev* 22: 1856–1864, 2008.
  3. **Barker N, van Es JH, Kuipers J, Kujala P, van den Born M, Cozijnsen M, Haegebarth A, Korving J, Begthel H, Peters PJ, Clevers H.** Identification of stem cells in small intestine and colon by marker gene *Lgr5*. *Nature* 449: 1003–1007, 2007.
  4. **Bernfield M, Götte M, Park PW, Reizes O, Fitzgerald ML, Lincecum J, Zako M.** Functions of cell surface heparan sulfate proteoglycans. *Annu Rev Biochem* 68: 729–777, 1999.
  5. **Bode L, Salvestrini C, Park PW, Li JP, Esko JD, Yamaguchi Y, Murch S, Freeze HH.** Heparan sulfate and syndecan-1 are essential in maintaining murine and human intestinal epithelial barrier function. *J Clin Invest* 118: 229–238, 2008.
  6. **Bornemann DJ, Duncan PE, Staatz W, Selleck S, Warrior R.** Abrogation of heparan sulfate synthesis in *Drosophila* disrupts the Wingless, Hedgehog and Decapentaplegic signaling pathways. *Development* 131: 1927–1938, 2004.
  7. **Bradley RS, Brown AM.** The proto-oncogene *int-1* encodes a secreted protein associated with the extracellular matrix. *EMBO J* 9: 1569–1575, 1990.
  8. **Bulow HE, Hobert O.** The molecular diversity of glycosaminoglycans shapes animal development. *Annu Rev Cell Dev Biol* 22: 375–407, 2006.
  9. **Cheng H, Leblond CP.** Origin, differentiation and renewal of the four main epithelial cell types in the mouse small intestine. III. Enterendocrine cells. *Am J Anat* 141: 503–519, 1974.
  10. **Cheng H, Leblond CP.** Origin, differentiation and renewal of the four main epithelial cell types in the mouse small intestine. II. Mucous cells. *Am J Anat* 141: 481–501, 1974.
  11. **Cheng H, Leblond CP.** Origin, differentiation and renewal of the four main epithelial cell types in the mouse small intestine. V. Unitarian Theory of the origin of the four epithelial cell types. *Am J Anat* 141: 537–561, 1974.
  12. **Cheng H, Leblond CP.** Origin, differentiation and renewal of the four main epithelial cell types in the mouse small intestine. I. Columnar cell. *Am J Anat* 141: 461–479, 1974.
  13. **Cheng H, Leblond CP.** Origin, differentiation and renewal of the four main epithelial cell types in the mouse small intestine. IV. Paneth cells. *Am J Anat* 141: 521–535, 1974.
  14. **Day R, Ilyas M, Daszak P, Talbot I, Forbes A.** Expression of syndecan-1 in inflammatory bowel disease and a possible mechanism of heparin therapy. *Dig Dis Sci* 44: 2508–2515, 1999.
  15. **Elenius K, Vainio S, Laato M, Salmivirta M, Thesleff I, Jalkanen M.** Induced expression of syndecan in healing wounds. *J Cell Biol* 114: 585–595, 1991.
  16. **el Marjou F, Janssen KP, Chang BH, Li M, Hindie V, Chan L, Louvard D, Chambon P, Metzger D, Robine S.** Tissue-specific and inducible Cre-mediated recombination in the gut epithelium. *Genesis* 39: 186–193, 2004.
  17. **Fang JY, Richardson BC.** The MAPK signaling pathways and colorectal cancer. *Lancet Oncol* 6: 322–327, 2005.
  18. **Freeman SD, Moore WM, Guiral EC, Holme AD, Turnbull JE, Pownall ME.** Extracellular regulation of developmental cell signaling by XtSulf1. *Dev Biol* 320: 436–445, 2008.
  19. **Gotoh N, Manova K, Tanaka S, Murohashi M, Hadari Y, Lee A, Hamada Y, Hiroe T, Ito M, Kurihara T, Nakazato H, Shibuya M, Lax I, Lacy E, Schlessinger J.** The docking protein FRS2 $\alpha$  is an essential component of multiple fibroblast growth factor responses during early mouse development. *Mol Cell Biol* 25: 4105–4116, 2005.
  20. **Hacker U, Nybakken K, Perrimon N.** Heparan sulfate proteoglycans: the sweet side of development. *Nat Rev Mol Cell Biol* 6: 530–541, 2005.
  21. **Hadari YR, Gotoh N, Kouhara H, Lax I, Schlessinger J.** Critical role for the docking-protein FRS2 $\alpha$  in FGF receptor-mediated signal transduction pathways. *Proc Natl Acad Sci USA* 98: 8578–8583, 2001.
  22. **Haltiwanger RS, Lowe JB.** Role of glycosylation in development. *Annu Rev Biochem* 73: 491–537, 2004.
  23. **Han C, Belenkaya TY, Khodoun M, Tauchi M, Lin X, Lin X.** Distinct and collaborative roles of *Drosophila* EXT family proteins in morphogen signalling and gradient formation. *Development* 131: 1563–1575, 2004.
  24. **He XC, Yin T, Grindley JC, Tian Q, Sato T, Tao WA, Dirisina R, Porter-Westpfahl KS, Hembree M, Johnson T, Wiedemann LM, Barrett TA, Hood L, Wu H, Li L.** PTEN-deficient intestinal stem cells initiate intestinal polyposis. *Nat Genet* 39: 189–198, 2007.
  25. **Hedgepeth CM, Conrad LJ, Zhang J, Huang HC, Lee VM, Klein PS.** Activation of the Wnt signaling pathway: a molecular mechanism for lithium action. *Dev Biol* 185: 82–91, 1997.
  26. **Inatani M, Irie F, Plump AS, Tessier-Lavigne M, Yamaguchi Y.** Mammalian brain morphogenesis and midline axon guidance require heparan sulfate. *Science* 302: 1044–1046, 2003.
  27. **Kirsch DG, Santiago PM, di Tomaso E, Sullivan JM, Hou WS, Dayton T, Jeffords LB, Sodha P, Mercer KL, Cohen R, Takeuchi O, Korsmeyer SJ, Bronson RT, Kim CF, Haigis KM, Jain RK, Jacks T.** p53 controls radiation-induced gastrointestinal syndrome in mice independent of apoptosis. *Science* 327: 593–596, 2010.
  28. **Klein PS, Melton DA.** A molecular mechanism for the effect of lithium on development. *Proc Natl Acad Sci USA* 93: 8455–8459, 1996.
  29. **Korinek V, Barker N, Moerer P, van Donselaar E, Huls G, Peters PJ, Clevers H.** Depletion of epithelial stem-cell compartments in the small intestine of mice lacking Tcf-4. *Nat Genet* 19: 379–383, 1998.
  30. **Koziel L, Kunath M, Kelly OG, Vortkamp A.** Ext1-dependent heparan sulfate regulates the range of Ihh signaling during endochondral ossification. *Dev Cell* 6: 801–813, 2004.
  31. **Lee G, Goretsky T, Managlia E, Dirisina R, Singh AP, Brown JB, May R, Yang GY, Ragheb JW, Evers BM, Weber CR, Turner JR, He XC, Katzman RB, Li L, Barrett TA.** Phosphoinositide 3-Kinase Signaling Mediates  $\beta$ -Catenin Activation in Intestinal Epithelial Stem and Progenitor Cells in Colitis. *Gastroenterology* 139: 869–881, 2010.
  32. **Lin X, Buff EM, Perrimon N, Michelson AM.** Heparan sulfate proteoglycans are essential for FGF receptor signaling during *Drosophila* embryonic development. *Development* 126: 3715–3723, 1999.
  33. **Lin X, Perrimon N.** Dally cooperates with *Drosophila* Frizzled to transduce Wingless signaling. *Nature* 400: 281–284, 1999.
  34. **Lin X, Wei G, Shi Z, Dryer L, Esko JD, Wells DE, Matzuk MM.** Disruption of gastrulation and heparan sulfate biosynthesis in EXT1-deficient mice. *Dev Biol* 224: 299–311, 2000.
  35. **Lind T, Tufaro F, McCormick C, Lindahl U, Lidholt K.** The putative tumor suppressors EXT1 and EXT2 are glycosyltransferases required for the biosynthesis of heparan sulfate. *J Biol Chem* 273: 26265–26268, 1998.
  36. **Lorentz O, Duluc I, Arcangelis AD, Simon-Assmann P, Kedinger M, Freund JN.** Key role of the *Cdx2* homeobox gene in extracellular matrix-mediated intestinal cell differentiation. *J Cell Biol* 139, 1553–1565, 1997.
  37. **McCormick C, Leduc Y, Martindale D, Mattison K, Esford LE, Dyer AP, Tufaro F.** The putative tumour suppressor EXT1 alters the expression of cell-surface heparan sulfate. *Nat Genet* 19: 158–161, 1998.
  38. **Muncan V, Sansom OJ, Tertoolen L, Phesse TJ, Begthel H, Sancho E, Cole AM, Gregorieff A, de Alboran IM, Clevers H, Clarke AR.** Rapid loss of intestinal crypts upon conditional deletion of the *Wnt/Tcf-4* target gene *c-Myc*. *Mol Cell Biol* 26: 8418–8426, 2006.
  39. **Nguyen HT, Dalmasso G, Yan Y, Laroui H, Dahan S, Mayer L, Sitarman SV, Merlin D.** MicroRNA-7 modulates CD98 expression during intestinal epithelial cell differentiation. *J Biol Chem* 285: 1479–1489, 2010.
  40. **Norton WH, Ledin J, Grandel H, Neumann CJ.** HSPG synthesis by zebrafish Ext2 and Extl3 is required for Fgf10 signalling during limb development. *Development* 132: 4963–4973, 2005.
  41. **Ohkawara B, Yamamoto TS, Tada M, Ueno N.** Role of glypican 4 in the regulation of convergent extension movements during gastrulation in *Xenopus laevis*. *Development* 130: 2129–2138, 2003.
  42. **Oshiro M, Ono K, Suzuki Y, Ota H, Katsuyama T, Mori N.** Immunohistochemical localization of heparan sulfate proteoglycan in human gastrointestinal tract. *Histochem Cell Biol* 115: 373–380, 2001.
  43. **Pellegrini L, Burke DF, von Delft F, Mulloy B, Blundell TL.** Crystal structure of fibroblast growth factor receptor ectodomain bound to ligand and heparin. *Nature* 407: 1029–1034, 2000.
  44. **Pinto D, Gregorieff A, Begthel H, Clevers H.** Canonical Wnt signals are essential for homeostasis of the intestinal epithelium. *Genes Dev* 17: 1709–1713, 2003.
  45. **Powell AE, Wang Y, Li Y, Poulin EJ, Means AL, Washington MK, Higginbotham JN, Juchheim A, Prasad N, Levy SE, Guo Y, Shyr Y, Aronow BJ, Haigis KM, Franklin JL, Coffey RJ.** The pan-ErbB negative regulator *Lrig1* is an intestinal stem cell marker that functions as a tumor suppressor. *Cell* 149: 146–158, 2012.
  46. **Reichsman F, Smith L, Cumberledge S.** Glycosaminoglycans can modulate extracellular localization of the wingless protein and promote signal transduction. *J Cell Biol* 135: 819–827, 1996.

47. Sangiorgi E, Capecchi MR. Bmi1 is expressed in vivo in intestinal stem cells. *Nat Genet* 40: 915–920, 2008.
48. Sarkar S, Floto RA, Berger Z, Imarisio S, Cordenier A, Pasco M, Cook LJ, Rubinsztein DC. Lithium induces autophagy by inhibiting inositol monophosphatase. *J Cell Biol* 170: 1101–1111, 2005.
49. Schlessinger J, Plotnikov AN, Ibrahim OA, Eliseenkova AV, Yeh BK, Yayon A, Linhardt RJ, Mohammadi M. Crystal structure of a ternary FGF-FGFR-heparin complex reveals a dual role for heparin in FGFR binding and dimerization. *Mol Cell* 6: 743–750, 2000.
50. Scoville DH, Sato T, He XC, Li L. Current view: intestinal stem cells and signaling. *Gastroenterology* 134: 849–864, 2008.
51. Stepp MA, Gibson HE, Gala PH, Iglesia DD, Pajoohesh-Ganji A, Pal-Ghosh S, Brown M, Aquino C, Schwartz AM, Goldberger O, Hinkes MT, Bernfield M. Defects in keratinocyte activation during wound healing in the syndecan-1-deficient mouse. *J Cell Sci* 115: 4517–4531, 2002.
52. Takei Y, Ozawa Y, Sato M, Watanabe A, Tabata T. Three Drosophila EXT genes shape morphogen gradients through synthesis of heparan sulfate proteoglycans. *Development* 131: 73–82, 2004.
53. Tao Q, Yokota C, Puck H, Kofron M, Birsoy B, Yan D, Asashima M, Wylie CC, Lin X, Heasman J. Maternal wnt11 activates the canonical wnt signaling pathway required for axis formation in *Xenopus* embryos. *Cell* 120: 857–871, 2005.
54. Toyoda H, Kinoshita-Toyoda A, Fox B, Selleck SB. Structural analysis of glycosaminoglycans in animals bearing mutations in sugarless, sulfateless, and tout-velu. *J Biol Chem* 275: 21856–21861, 2000.
55. Tsuda M, Kamimura K, Nakato H, Archer M, Staatz W, Fox B, Humphrey M, Olson S, Futch T, Kaluza V, Siegfried E, Stam L, Selleck SB. The cell-surface proteoglycan Dally regulates Wingless signalling in *Drosophila*. *Nature* 400: 276–280, 1999.
56. Vidrich A, Buzan JM, Brodrick B, Ilo C, Bradley L, Fendig KS, Sturgill T, Cohn SM. Fibroblast growth factor receptor-3 regulates Paneth cell lineage allocation and accrual of epithelial stem cells during murine intestinal development. *Am J Physiol Gastrointest Liver Physiol* 297: G168–G178, 2009.
57. Wang L, Srinivasan S, Theiss AL, Merlin D, Sitaraman SV. Interleukin-6 induces keratin expression in intestinal epithelial cells: potential role of keratin-8 in interleukin-6-induced barrier function alterations. *J Biol Chem* 282: 8219–8227, 2007.
58. Whitelock JM, Iozzo RV. Heparan sulfate: a complex polymer charged with biological activity. *Chem Rev* 105: 2745–2764, 2005.
59. Withers HR, Elkind MM. Microcolony survival assay for cells of mouse intestinal mucosa exposed to radiation. *Int J Radiat Biol Relat Stud Phys Chem Med* 17: 261–267, 1970.

